## Supplemental Information

## Supplemental Methods

**Histology and immunohistochemistry.** *Human samples:* A portion of each core was vacuum embedded in 50:50 O.C.T. (Sakura) and PBS or paraffin then sectioned for histology with additional samples cut for gene expression. Hematoxylin and eosin (H&E) stain was used for Ashcroft scoring (1) of the extent of fibrosis within the sample. Samples with emphysema, large vessels, or airways were excluded. Cryosections were stained with picrosirius red for total collagen and Van Gieson for elastin; antibodies were used to detect collagen type I (ab6308; Abcam, USA), collagen type III (2150-0100; Bio-Rad, USA). Paraffin sections were used to detect POU2AF1/BOB1 (ab238036; Abcam, USA). Slides were imaged using an Aperio digital pathology slide scanner (Leica Biosystems Inc., Canada) and quantified with Aperio Image Analysis software. Segmentation of positively stained tissue and total tissue were used to determine the volume fraction (Vv) of staining for each marker. Surface density was found to have highest correlation with Ashcroft scores and was used for downstream analyses (*SI Appendix*, Figure 1*A*). *Mouse samples:* Paraffin-embedded tissue sections were stained with Masson's trichrome (collagen/connective tissue) or H&E using two slices per animal and two animals per group. Immunohistochemistry for α-smooth muscle actin (α-SMA) (ab5694; Abcam, USA) was performed with non-immune serum used for negative controls.

**mRNA-sequencing and microRNA analysis.** RNA was extracted using miRNeasy mini kit (Qiagen) from each core according the manufacturer's protocol. RNA concentration and integrity were measured by using NanoDrop ND-2000 and 2200 Tape Station. 20 ng RNA input was used for RNA sequencing per sample, using Ion AmpliSeq™ Transcriptome Human Gene Expression kit according the manufacturer's protocol. The cDNA was then amplified and barcoded using the Ion Xpress™ RNA-Seq Barcode 1-16 Kit (Life Technologies 4475485). The Ion PI™ Chip Kit v2 BC (Life Technologies 4484270) was then loaded using the Ion Chef™ System (Life Technologies 4484177) with the Ion PI™ IC 200 Kit (Life Technologies 4488377). Afterwards, the chips were run on the Ion Proton™ System for Next-Generation Sequencing (Life Technologies 4476610) Fastq files after quality control for adapter contamination and trimming, were mapped on human genome by combinations of Tophat and Bowtie2 softwares. Cufflinks was used to calculate the Fragments per Kilobase of transcript per Million mapped reads (FPKM) values as the estimated gene expression levels.

MicroRNA evaluation was performed on all samples using 50 ng total RNA using the nCounter Analysis System (NanoString Technologies) and Comprehensive NanoString pre-built miRNA panels for human (HumanV2.1 miRNA Assay) contains 800 unique miRNA barcodes were utilized. Probes for several housekeeping genes such as Ribosomal protein L10 (RPL10), β-actin (ACTB), β-2-microglobulin (B2M), glyceraldehyde 3-phosphate dehydrogenase (GAPDH), and ribosomal protein L19 (RPL19), as well as for endogenous miRNAs are incorporated in the Nanostring codesets and were used for analysis along with positive and negative controls. Data normalization was performed using nSolver, an analysis software provided by Nanostring.

**Differential expression analysis.** The 25,276 genes were filtered to remove low and non-expressing genes with expression below 0.01 FPKM in more than 90% of samples resulting in 21,804 genes remaining. Samples were log2 transformed and divided based on principal component analysis of microCT surface density measurements and collagen 1 and collagen 3 immunostaining volume fractions followed by expectation-maximization clustering into three groups representing early stage disease with normal lung structure (IPF1), moderate stage disease where progressive changes are occurring (IPF2), and late stage disease with severe fibrosis and end-stage pathology (IPF3). Two linear mixed-effects models were used to identify differential gene expression profiles in each of these groups:

1. $Gene_{ij} = \beta_0 + \alpha_{SLICE} + \alpha_j + \varepsilon_{ij}$
2. $Gene_{ij} = \beta_0 + DISEASE_{ij} + \alpha_{SLICE} + \alpha_j + \varepsilon_{ij}$

$i = 1, 2, \ldots, 6$; $j = 1, 2, \ldots, 16$

$Gene_{ij}$ is the log2 transformed FPKM expression value for sample *i* in subject *j* for a single gene. “SLICE” is a random effect controlling for the location the sample was collected and differences in lung size between control and IPF lungs. $\alpha_j$ represents the random effect for each subject with $\beta_0$ representing the intercept and $\varepsilon_{ij}$ the random error. Model 2 includes the fixed effects of “DISEASE” and ANOVA was used to compare the two models. A false discovery rate (FDR) adjusted P-value $< 0.05$ was considered significant. The same model was applied to the microRNA data to determine differential microRNA expression with an adjusted P-value $< 0.1$. All statistical analyses were conducted using R statistical software (v.3.3.2) and the *lme4* package.

**Dynamic regulatory events miner**. We applied the dynamic regulatory event miner (DREM) (2, 3) to our dataset to develop a model of regulatory tracks associated with disease progression in IPF. Briefly, DREM integrates transcription factor and microRNA binding interactions and time-series gene expression data to reconstruct dynamic regulatory networks by identifying bifurcation events, places in the time-series where a set of genes that were previously co-expressed diverges. DREM annotates these split events with TFs and microRNAs that are predicted to regulate genes in the outgoing upward and/or downward tracks allowing us to associate temporal or stage information (the timing of the splits) with the static regulator-DNA interaction data. An input-output hidden Markov model (IOHMM) (4), which unlike traditional HMMs also includes additional observed (in our case static) input data that can influence transition probabilities, was used to obtained the underlying probabilistic graphical model. In the DREM IOHMM, regulator-target interactions serve as the static input data that influence transitions between hidden states. An L1-regularized logistic regression classifier was trained at all expression profile bifurcations to assign transition probabilities to genes based on the set of TFs and microRNAs that bind them. DREM searches the state space of possible splits in gene expression profiles to predict a compact set of diverging gene expression tracks and the regulators that control them, ranking these regulators by order of importance. DREM has been successfully applied to reconstruct networks in a large number of species (5). Furthermore, using gene markers for annotated cell types from a publicly available single cell RNA-seq dataset of lung tissues (6), we were able to map the association of specific lung cells to each of the DREM tracks.

**Mouse model of lung fibrosis.** C57BL/6 wild-type mice (WT) were obtained from Jackson Laboratory (Bar Harbor, ME). Pou2af1$^{-/-}$ mice (KO) on the C57BL/6 background were from the University of Utah (7). Eight- to 12-week-old female mice were randomly assigned groups and administered either 3.0 U/kg bleomycin (Hospira Inc., Lake Forest, IL) or an equivalent volume (50 µL) of 0.9% saline intratracheally as control and sacrificed at day 14. A total of 104 mice from 3 batches were used in this study (WT-saline (WTS), n = 26;

WT-bleomycin (WTB), n = 26; KO-saline (KOS), n = 23; KO-bleomycin (KOB), n = 29). All animal included in this study were approved by the Institutional Animal Care and Use Committee (IACUC) at Yale University (2016-20084).

**Mouse lung RNA extraction.** Total RNA was extracted from 30-50 mg of frozen lung tissue in 700 µL Qiazol lysis buffer (Qiagen, Valencia, CA, USA) by tissue disruption and homogenization using an electric homogenizer (PolyTron homogenizer H3660-2A, Cardinal Health, Dublin, OH, USA) according to the manufacturer's instructions. RNA was purified using the miRNeasy Mini kit (217004, Qiagen, Valencia, CA, USA) with Qiacube automated system (9001292, Qiagen, Valencia, CA, USA). The purity of the RNA was verified by NanoDrop (Thermo Fisher Scientific Inc., Wilmington, DE, USA) at 260 nm and the quality of the RNA was assessed using the Agilent 2100 Bioanalyzer (Agilent Technologies, Santa Clara, CA, USA).

**Quantitative Real-Time PCR.** Gene expression was determined by employing TaqMan (Life Technologies, Thermo Scientific Inc. Rockford, IL, USA) according to manufacturer's instruction. The real-time PCR reaction mix were made by TaqMan RNA to-CT 1-step kit (Taqman®, Life Technologies, Thermo Scientific Inc. Rockford, IL, USA) and proceeded with Viia real-time PCR System (Life Technologies, Thermo Scientific Inc. Rockford IL, USA). β-glucuronidase (Gusb) was employed as an internal standard control and Collagen I α1 primer was obtained from Life Technologies (Thermo Scientific Inc. Rockford, IL, USA). Each reaction was performed in triplicate. Relative gene expression was then normalized to the unstimulated control group. Control reactions without RNA were performed as negative control. A linear mixed-effects model was used to compare relative expression of Col1A1 between groups with the batch as a random effect.

**Hydroxyproline assay.** Lung hydroxyproline content was analyzed with hydroxyproline colorimetric assay kit (BioVision Inc, Milpitas, CA) following manufacturer's instruction. The lungs from control and experimental mice were hydrolyzed in 12N HCl for 3 h at 120°C. The digestions reacted with Chloramine T reagent and visualized in DMAB reagent. The absorbance was measured at 560 nm in a microplate reader and the micrograms of hydroxyproline per right lung was calculated. Each assay was then normalized to the unstimulated control group. A linear mixed-effects model was used to compare relative hydroxyproline levels between groups with the batch as a random effect.

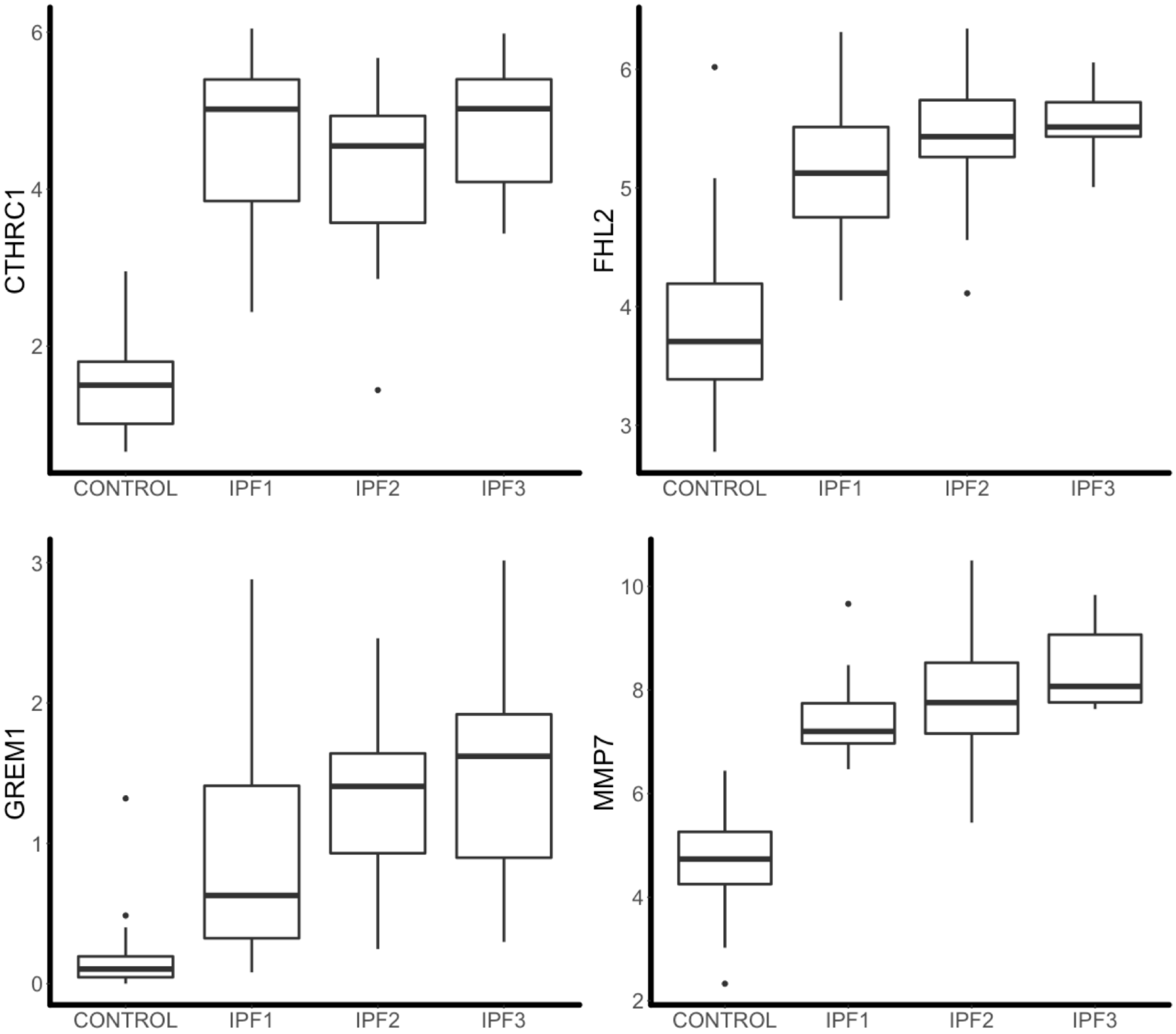

**Figure S1.** Four genes were found to be related to disease progression in IPF identified in a previous study (8). Three of these genes (FHL2, GREM1, and MMP7) showed expression increased in our samples as disease stages become more advanced while CTHRC1 showed consistently high expression at all disease stages.

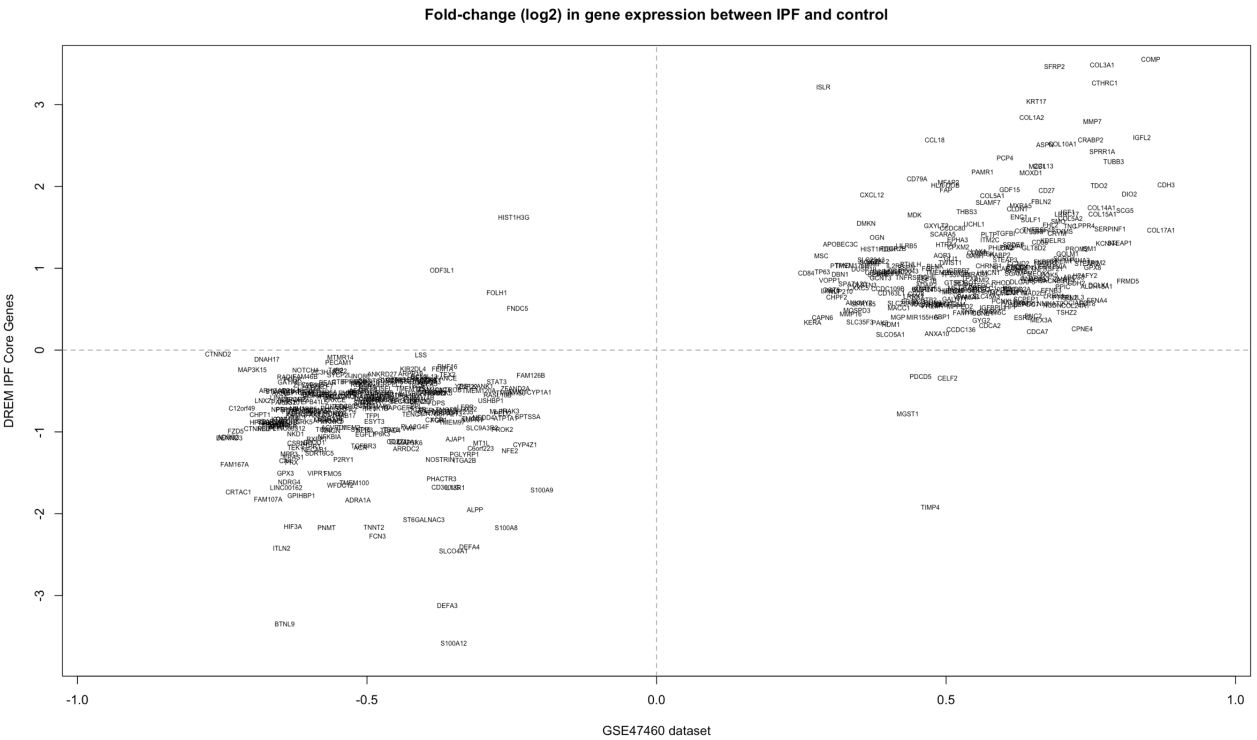

**Figure S2.** Direction of expression of core genes compared with differentially expressed genes from the LTRC dataset GSE47460 used in a previously published study (9).

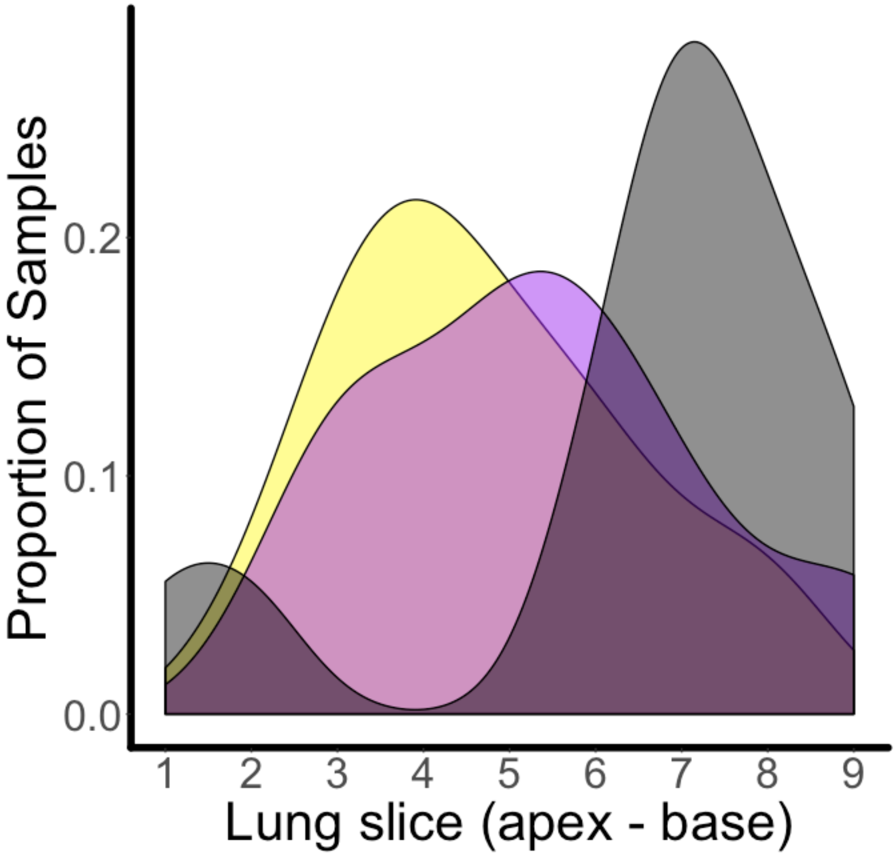

**Figure S3:** Distribution of samples for each fibrosis severity group according to lung slice measured from apex to base of the lung. As expected for IPF, we found apical regions of the lung were less severely fibrotic (IPF1) compared to basal regions of the lung which were comprised mainly of the severe fibrotic group (IPF3). IPF1 = yellow, IPF2 = purple, IPF3 = black.

**Table S1:** Top 100 differentially expressed genes (up or down-regulated) in IPF. Foldchange (fc) refers to log2 fold-change of each gene for that IPF stage versus control. Red boxes highlight the adjusted p-values that were below the significance threshold (0.05).

| Gene ID | IPF1_adj.pval | IPF2_adj.pval | IPF3_adj.pval | IPF1_fc | IPF2_fc | IPF3_fc | Track |
|---|---|---|---|---|---|---|---|
| ADRA1A | 4.89E-04 | 2.29E-05 | 4.46E-04 | -1.9 | -2.1 | -2.0 | track_M |
| AGER | 1.07E-01 | 3.42E-02 | 1.74E-02 | -1.3 | -2.0 | -2.5 | track_M |
| ALPP | 6.52E-03 | 5.34E-03 | 3.83E-03 | -2.1 | -2.2 | -2.1 | track_M |
| APLNR | 1.03E-01 | 2.53E-02 | 2.95E-01 | 1.4 | 1.4 | 2.3 | track_B |
| ASPN | 4.89E-04 | 1.26E-03 | 4.02E-04 | 2.4 | 2.2 | 2.3 | track_A |
| BPIFB1 | 5.98E-01 | 4.67E-02 | 1.86E-02 | 0.8 | 2.3 | 2.7 | track_A |
| BTNL9 | 5.58E-04 | 8.10E-05 | 1.91E-04 | -3.5 | -4.3 | -3.6 | track_M |
| CA4 | 1.03E-02 | 2.71E-04 | 2.13E-03 | -1.5 | -2.8 | -2.5 | track_M |
| CCL13 | 1.89E-02 | 1.33E-02 | 3.96E-02 | 2.1 | 2.3 | 2.2 | track_A |
| CCL18 | 1.41E-02 | 1.82E-02 | 3.20E-02 | 2.5 | 2.1 | 2.2 | track_A |
| CD27 | 8.54E-03 | 1.15E-04 | 8.66E-04 | 1.8 | 2.2 | 2.1 | track_A |
| CD300LG | 4.86E-02 | 2.57E-02 | 1.51E-02 | -1.8 | -2.2 | -2.0 | track_M |
| CD79A | 2.70E-02 | 5.76E-04 | 1.50E-03 | 2.0 | 2.6 | 2.7 | track_A |
| CDH3 | 3.98E-04 | 1.64E-05 | 2.50E-05 | 1.9 | 2.3 | 2.4 | track_A |
| CHI3L2 | 5.26E-02 | 4.84E-02 | 2.52E-02 | -2.1 | -2.0 | -2.4 | track_M |
| CLEC1B | 8.28E-02 | 1.40E-02 | 1.17E-02 | -1.7 | -2.3 | -2.4 | track_M |
| CLEC4E | 3.57E-03 | 1.24E-03 | 4.53E-04 | -2.1 | -2.6 | -2.8 | track_M |
| COL10A1 | 4.46E-03 | 6.11E-03 | 1.06E-04 | 2.4 | 2.1 | 2.3 | track_A |
| COL15A1 | 1.76E-02 | 3.36E-03 | 1.65E-03 | 1.5 | 1.8 | 2.3 | track_B |
| COL1A1 | 4.71E-03 | 1.43E-04 | 6.73E-05 | 4.0 | 3.8 | 4.3 | track_A |
| COL1A2 | 4.20E-03 | 1.36E-04 | 3.24E-04 | 2.7 | 2.5 | 2.8 | track_A |
| COL2A1 | 3.47E-02 | 8.14E-04 | 4.48E-05 | 2.0 | 1.9 | 2.4 | track_B |
| COL3A1 | 1.28E-03 | 1.64E-05 | 1.49E-05 | 3.4 | 3.0 | 3.5 | track_A |
| COL5A1 | 3.95E-02 | 1.57E-03 | 6.99E-04 | 1.8 | 1.7 | 2.2 | track_B |
| COMP | 9.93E-03 | 3.39E-03 | 8.11E-04 | 3.4 | 3.1 | 3.4 | track_A |
| CPXM1 | 2.52E-01 | 6.50E-05 | 2.12E-05 | 0.9 | 1.9 | 3.0 | track_A |
| CRABP2 | 7.94E-03 | 1.36E-03 | 3.09E-04 | 2.5 | 2.9 | 3.1 | track_A |
| CST2 | 1.10E-02 | 1.41E-02 | 3.35E-03 | 2.8 | 2.6 | 2.5 | track_A |
| CTHRC1 | 1.79E-03 | 1.17E-04 | 1.53E-05 | 3.1 | 2.6 | 3.3 | track_A |
| CXCL13 | 6.09E-02 | 3.67E-03 | 3.93E-03 | 2.0 | 2.7 | 3.2 | track_A |
| CXCL14 | 4.89E-04 | 8.10E-05 | 1.46E-04 | 3.0 | 3.3 | 3.4 | track_A |
| CXCL6 | 2.60E-01 | 1.20E-02 | 1.15E-02 | 1.4 | 2.6 | 2.7 | track_A |
| DEFA1 | 1.10E-02 | 6.46E-03 | 3.00E-03 | -3.4 | -4.0 | -3.6 | track_M |
| DEFA3 | 2.29E-02 | 1.31E-02 | 8.64E-03 | -3.2 | -3.8 | -3.5 | track_M |

| | | | | | | | |
|---|---|---|---|---|---|---|---|
| DEFA4 | 1.89E-02 | 9.05E-03 | 8.60E-03 | -2.5 | -2.6 | -2.6 | track_M |
| F2RL3 | 2.73E-02 | 8.83E-03 | 2.79E-03 | -2.3 | -3.0 | -3.0 | track_M |
| FAM107A | 1.91E-02 | 4.17E-02 | 4.02E-03 | -1.9 | -2.5 | -2.4 | track_M |
| FAP | 2.60E-03 | 9.96E-05 | 2.12E-05 | 1.8 | 1.6 | 2.3 | track_B |
| FCN3 | 2.37E-02 | 8.59E-03 | 2.67E-03 | -2.4 | -3.2 | -2.8 | track_M |
| FOLR2 | 2.84E-04 | 8.10E-05 | 3.40E-03 | 2.2 | 1.8 | 1.7 | track_B |
| GGTLC1 | 1.72E-01 | 4.57E-02 | 2.96E-02 | -1.3 | -2.0 | -2.4 | track_M |
| GP9 | 2.06E-01 | 1.80E-02 | 3.33E-02 | -1.3 | -2.2 | -2.0 | track_M |
| GSTA1 | 3.95E-01 | 6.17E-02 | 3.29E-02 | 1.0 | 1.8 | 2.1 | track_B |
| GSTA2 | 1.66E-01 | 2.05E-02 | 1.21E-02 | 1.5 | 2.2 | 2.5 | track_A |
| HBA1 | 2.73E-02 | 4.34E-02 | 1.20E-01 | 3.5 | 2.6 | 2.5 | track_A |
| HBA2 | 2.72E-02 | 4.19E-02 | 1.05E-01 | 3.5 | 2.6 | 2.5 | track_A |
| HBB | 3.15E-02 | 5.14E-02 | 1.07E-01 | 3.5 | 2.7 | 2.6 | track_A |
| HIF3A | 1.29E-02 | 6.65E-03 | 3.81E-02 | -2.3 | -2.6 | -2.0 | track_M |
| HLA-DOB | 6.27E-03 | 4.26E-04 | 6.75E-04 | 1.9 | 2.1 | 2.2 | track_A |
| IGFL2 | 1.28E-03 | 1.11E-03 | 2.73E-05 | 2.5 | 2.9 | 2.7 | track_A |
| IGJ | 2.68E-02 | 4.86E-02 | 7.83E-02 | 2.1 | 2.1 | 1.8 | track_B |
| IGLL5 | 6.84E-03 | 3.60E-03 | 8.60E-03 | 3.3 | 3.7 | 3.3 | track_A |
| IL1R2 | 6.68E-02 | 4.38E-02 | 2.87E-02 | -2.6 | -2.6 | -2.6 | track_M |
| ISLR | 1.17E-03 | 4.57E-05 | 1.24E-05 | 3.1 | 3.0 | 3.4 | track_A |
| ITLN2 | 1.74E-02 | 1.94E-04 | 2.79E-03 | -2.5 | -3.1 | -3.4 | track_M |
| KRT14 | 1.48E-01 | 1.15E-02 | 1.41E-02 | 2.0 | 3.1 | 2.8 | track_A |
| KRT15 | 3.87E-01 | 8.38E-03 | 1.09E-02 | 0.8 | 1.9 | 2.1 | track_B |
| KRT17 | 5.26E-03 | 9.84E-05 | 9.99E-05 | 2.9 | 4.0 | 4.0 | track_A |
| KRT5 | 3.36E-01 | 8.93E-03 | 1.26E-02 | 1.3 | 2.7 | 2.9 | track_A |
| LINC00162 | 1.37E-02 | 8.21E-03 | 3.04E-03 | -1.8 | -1.9 | -2.4 | track_M |
| LY6D | 1.02E-01 | 1.17E-04 | 2.19E-02 | 0.6 | 2.3 | 2.0 | track_A |
| LY6G6F | 6.21E-02 | 1.51E-02 | 2.46E-02 | -1.6 | -2.3 | -2.0 | track_M |
| MMP11 | 5.17E-02 | 5.01E-03 | 1.67E-02 | 1.7 | 2.2 | 2.5 | track_A |
| MMP7 | 1.06E-03 | 9.84E-05 | 1.53E-05 | 2.7 | 3.5 | 3.6 | track_A |
| MOXD1 | 4.91E-03 | 7.95E-04 | 7.43E-04 | 2.1 | 1.8 | 2.4 | track_B |
| MT1A | 4.41E-02 | 2.71E-02 | 2.85E-03 | -2.5 | -2.5 | -3.2 | track_M |
| MT1M | 8.49E-02 | 3.15E-02 | 3.15E-02 | -2.6 | -3.1 | -3.0 | track_M |
| MZB1 | 3.26E-02 | 3.98E-03 | 3.40E-03 | 2.1 | 2.7 | 2.9 | track_A |
| NDRG4 | 1.28E-03 | 9.96E-05 | 1.63E-05 | -1.7 | -2.1 | -2.3 | track_M |
| PAMR1 | 1.11E-03 | 3.41E-04 | 2.12E-05 | 2.1 | 1.7 | 2.2 | track_B |
| PCP4 | 2.90E-02 | 2.90E-02 | 2.79E-02 | 2.2 | 1.9 | 2.3 | track_B |
| PF4 | 1.31E-01 | 1.73E-02 | 2.78E-02 | -2.1 | -3.4 | -3.0 | track_M |
| PNMT | 2.43E-02 | 7.90E-03 | 1.71E-02 | -2.3 | -2.5 | -2.3 | track_M |
| POSTN | 2.24E-02 | 1.57E-03 | 1.24E-03 | 2.3 | 2.3 | 2.5 | track_A |

| | | | | | | | |
|---|---|---|---|---|---|---|---|
| POU2AF1 | 5.29E-02 | 2.61E-03 | 1.30E-03 | 1.3 | 1.9 | 2.2 | track_B |
| S100A12 | 3.98E-04 | 2.46E-04 | 1.53E-05 | -3.7 | -3.2 | -3.6 | track_M |
| S100A2 | 2.02E-01 | 1.58E-03 | 2.37E-03 | 1.5 | 2.9 | 3.2 | track_A |
| S100A8 | 4.89E-04 | 4.26E-04 | 2.39E-04 | -2.3 | -2.3 | -2.8 | track_M |
| S100A9 | 7.59E-03 | 9.09E-03 | 3.90E-03 | -1.8 | -2.1 | -2.2 | track_M |
| SERPINB3 | 4.12E-01 | 2.06E-02 | 3.26E-02 | 1.1 | 2.3 | 2.6 | track_A |
| SERPIND1 | 1.64E-02 | 6.33E-05 | 1.30E-03 | 2.2 | 2.9 | 2.5 | track_A |
| SFRP2 | 4.89E-04 | 3.25E-04 | 1.24E-04 | 3.4 | 3.1 | 3.1 | track_A |
| SFRP4 | 5.13E-04 | 6.61E-03 | 1.98E-02 | 3.2 | 2.2 | 2.7 | track_A |
| SLCO4A1 | 3.09E-03 | 5.54E-03 | 2.48E-04 | -2.6 | -2.3 | -2.7 | track_M |
| SNORD83B | 1.83E-01 | 4.82E-02 | 7.09E-01 | -1.9 | -2.3 | -0.6 | track_M |
| SPP1 | 2.29E-01 | 3.64E-02 | 9.79E-03 | 1.4 | 2.5 | 2.6 | track_A |
| SPRR1A | 8.83E-03 | 9.97E-03 | 8.11E-04 | 2.3 | 2.5 | 2.9 | track_A |
| SPRR1B | 2.33E-01 | 6.89E-01 | 1.21E-02 | 0.6 | 0.6 | 2.3 | track_B |
| ST6GALNAC3 | 3.09E-03 | 5.14E-04 | 5.64E-04 | -2.2 | -2.1 | -2.1 | track_M |
| SULF1 | 1.94E-03 | 3.25E-04 | 4.48E-05 | 1.5 | 1.7 | 2.2 | track_B |
| TDO2 | 8.66E-03 | 1.21E-03 | 2.69E-03 | 1.9 | 2.5 | 2.4 | track_A |
| THBS2 | 1.75E-02 | 2.09E-04 | 3.62E-04 | 2.0 | 2.0 | 2.7 | track_A |
| THY1 | 1.53E-03 | 2.71E-04 | 7.49E-04 | 3.8 | 3.7 | 3.8 | track_A |
| TIMP4 | 7.97E-03 | 1.51E-02 | 2.45E-03 | -2.0 | -1.6 | -2.1 | track_M |
| TMEM100 | 6.72E-03 | 1.58E-02 | 3.85E-04 | -1.7 | -2.1 | -2.8 | track_M |
| TNNT2 | 4.89E-04 | 1.21E-03 | 9.01E-04 | -2.3 | -2.1 | -1.9 | track_M |
| TTR | 1.80E-02 | 8.38E-03 | 9.11E-02 | 2.9 | 1.4 | 2.0 | track_B |
| TUBB3 | 4.20E-03 | 1.64E-05 | 8.76E-05 | 2.2 | 2.4 | 2.5 | track_A |
| UBD | 8.06E-02 | 4.61E-02 | 4.62E-02 | 2.0 | 2.0 | 2.1 | track_B |
| VIPR1 | 3.28E-03 | 5.16E-04 | 4.18E-04 | -1.6 | -2.2 | -2.3 | track_M |

**Table S2:** Table of the 69 genes identified as relevant to IPF.(10) Half the genes (34/69) were found to be differentially expressed in at least one stage in our dataset. Of these genes 16 were differentially expressed at all stages of disease while 14 were at the late stages of disease. Four genes were expressed in both the early and late stage but were above the significance threshold to be a core gene.

| GENE | IPF1_adj.p.val | IPF2_adj.pv.al | IPF3_adj.p.val | IPF1_fc | IPF2_fc | IPF3_fc | Track |
|---|---|---|---|---|---|---|---|
| AGER | 1.07E-01 | 3.42E-02 | 1.74E-02 | -1.263 | -2.007 | -2.536 | track_M |
| BAX | 7.28E-02 | 5.49E-02 | 7.31E-02 | 0.509 | 0.502 | 0.421 | #N/A |
| BPIFA1 | 8.40E-01 | 1.77E-01 | 1.62E-01 | 0.450 | 1.712 | 1.897 | #N/A |
| C6 | 8.95E-01 | 5.16E-01 | 3.81E-01 | 0.106 | 0.347 | 0.422 | #N/A |
| CASP6 | 7.25E-01 | 4.13E-01 | 4.03E-01 | 0.126 | 0.228 | 0.216 | #N/A |
| CAV1 | 9.23E-01 | 9.12E-01 | 7.71E-01 | -0.037 | 0.047 | 0.117 | #N/A |
| CCNA2 | 2.60E-01 | 1.51E-01 | 3.19E-02 | 0.358 | 0.399 | 0.608 | track_E |
| CDH2 | 1.50E-02 | 1.09E-02 | 1.54E-03 | 0.701 | 0.905 | 0.890 | track_C |
| COMP | 9.93E-03 | 3.39E-03 | 8.11E-04 | 3.438 | 3.060 | 3.376 | track_A |
| CRLF1 | 2.37E-02 | 1.26E-02 | 1.16E-02 | 1.774 | 1.775 | 1.714 | track_B |
| CTHRC1 | 1.79E-03 | 1.17E-04 | 1.53E-05 | 3.147 | 2.628 | 3.331 | track_A |
| CTNNB1 | 5.98E-01 | 4.18E-01 | 6.96E-01 | 0.118 | 0.125 | 0.066 | #N/A |
| CTSE | 3.78E-02 | 1.05E-02 | 7.34E-02 | 1.378 | 1.464 | 1.225 | track_B |
| CXCL12 | 2.31E-02 | 3.67E-03 | 8.60E-03 | 1.784 | 2.046 | 2.008 | track_B |
| DEFA3 | 2.29E-02 | 1.31E-02 | 8.64E-03 | -3.239 | -3.767 | -3.460 | track_M |
| DEFA4 | 1.89E-02 | 9.05E-03 | 8.60E-03 | -2.524 | -2.618 | -2.559 | track_M |
| DIO2 | 1.22E-02 | 8.33E-05 | 6.47E-05 | 1.792 | 1.707 | 2.025 | track_B |
| DNAH6 | 9.50E-01 | 1.76E-01 | 1.39E-01 | -0.025 | 0.498 | 0.536 | #N/A |
| DNAH7 | 9.23E-01 | 1.90E-01 | 1.73E-01 | 0.044 | 0.458 | 0.413 | #N/A |
| DNAI1 | 8.33E-01 | 1.44E-01 | 7.16E-02 | 0.195 | 0.861 | 1.083 | #N/A |
| EGFR | 5.51E-02 | 2.75E-02 | 3.29E-02 | -0.528 | -0.602 | -0.468 | track_J |
| FHL2 | 4.59E-03 | 1.42E-03 | 5.96E-04 | 1.414 | 1.558 | 1.666 | track_B |
| FKBP10 | 1.06E-01 | 1.03E-01 | 2.68E-02 | 0.924 | 0.762 | 1.032 | track_C |
| FOXF1 | 1.55E-01 | 1.06E-02 | 1.28E-02 | -0.655 | -1.110 | -1.144 | track_L |
| FZD2 | 9.51E-01 | 1.00E+00 | 8.44E-01 | 0.040 | 0.002 | 0.135 | #N/A |
| FZD3 | 9.84E-01 | 3.61E-01 | 1.05E-01 | 0.005 | 0.142 | 0.214 | #N/A |
| GAL | 8.24E-01 | 1.10E-01 | 2.28E-01 | 0.071 | 0.502 | 0.293 | #N/A |
| GREM1 | 4.93E-02 | 3.41E-04 | 1.99E-02 | 0.974 | 1.172 | 1.264 | track_C |
| GSK3B | 4.07E-01 | 4.74E-01 | 2.89E-01 | -0.181 | -0.146 | -0.236 | #N/A |
| HIF1A | 8.85E-01 | 3.21E-01 | 5.06E-01 | 0.052 | 0.404 | 0.223 | #N/A |

| | | | | | | | |
|---|---|---|---|---|---|---|---|
| HSPA1A | 1.15E-01 | 9.00E-01 | 7.34E-02 | 0.563 | 0.052 | 0.491 | #N/A |
| IGFBP3 | 2.59E-01 | 5.00E-01 | 2.17E-01 | 0.872 | 0.595 | 0.836 | #N/A |
| IGFBP4 | 1.86E-01 | 1.69E-02 | 5.23E-02 | 0.609 | 1.041 | 0.890 | track_C |
| IGFBP5 | 3.01E-01 | 1.05E-01 | 3.16E-02 | 0.541 | 0.759 | 0.890 | track_D |
| LCLAT1 | 9.90E-01 | 4.87E-01 | 4.91E-01 | 0.005 | 0.182 | 0.167 | #N/A |
| LCN2 | 7.88E-01 | 1.83E-01 | 1.25E-01 | 0.279 | 1.058 | 1.186 | #N/A |
| LEF1 | 2.63E-02 | 8.82E-02 | 3.40E-03 | 0.507 | 0.564 | 0.522 | track_E |
| LRP5 | 9.33E-01 | 9.61E-01 | 8.42E-01 | -0.048 | 0.024 | 0.085 | #N/A |
| MMP1 | 6.81E-01 | 4.52E-03 | 2.01E-03 | 0.278 | 1.320 | 1.688 | track_B |
| MMP19 | 1.23E-02 | 1.46E-01 | 1.16E-02 | 1.196 | 0.918 | 1.274 | track_C |
| MMP2 | 4.20E-02 | 2.82E-02 | 1.11E-02 | 1.410 | 1.159 | 1.563 | track_B |
| MMP28 | 9.45E-01 | 4.57E-01 | 4.70E-01 | -0.040 | -0.358 | -0.247 | #N/A |
| MMP3 | 7.17E-01 | 9.96E-01 | 3.03E-01 | -0.011 | 0.000 | 0.031 | #N/A |
| MMP7 | 1.06E-03 | 9.84E-05 | 1.53E-05 | 2.680 | 3.455 | 3.648 | track_A |
| MMP9 | 2.37E-01 | 8.09E-01 | 3.05E-01 | 1.329 | 0.340 | 0.815 | #N/A |
| MUC5B | 2.35E-01 | 1.29E-02 | 1.47E-02 | 1.046 | 1.632 | 1.875 | track_B |
| NELL1 | 2.38E-01 | 1.75E-01 | 3.14E-01 | 0.129 | 0.147 | 0.107 | #N/A |
| PCSK1 | 3.78E-01 | 1.99E-02 | 9.72E-03 | 0.096 | 0.163 | 0.229 | track_G |
| PINK1 | 9.81E-01 | 4.45E-01 | 7.50E-01 | 0.011 | -0.243 | -0.098 | #N/A |
| PLA2G2A | 1.64E-01 | 7.14E-02 | 9.76E-02 | 1.186 | 1.371 | 1.232 | #N/A |
| PTPN11 | 1.44E-01 | 1.38E-01 | 7.71E-02 | -0.366 | -0.251 | -0.309 | #N/A |
| RPGRIP1L | 8.85E-01 | 2.68E-01 | 1.63E-01 | 0.050 | 0.304 | 0.367 | #N/A |
| RXFP1 | 1.88E-02 | 1.74E-03 | 3.25E-03 | -1.205 | -1.326 | -1.434 | track_L |
| SERPINF1 | 8.36E-03 | 3.09E-03 | 1.55E-03 | 1.363 | 1.331 | 1.480 | track_B |
| SFTPA1 | 1.91E-01 | 1.64E-01 | 9.35E-02 | -0.563 | -0.700 | -0.867 | #N/A |
| SLC2A5 | 1.94E-01 | 8.96E-02 | 2.88E-02 | 0.402 | 0.625 | 0.716 | track_D |
| SPP1 | 2.29E-01 | 3.64E-02 | 9.79E-03 | 1.382 | 2.523 | 2.558 | track_A |
| SYN2 | 3.03E-02 | 1.10E-02 | 1.35E-02 | -1.119 | -1.277 | -1.190 | track_L |
| TAGLN | 8.95E-01 | 1.61E-01 | 5.08E-01 | 0.079 | 0.562 | 0.275 | #N/A |
| TAZ | 5.36E-01 | 9.00E-01 | 9.55E-01 | -0.289 | -0.069 | 0.034 | #N/A |
| TNFSF10 | 9.32E-01 | 6.86E-01 | 8.07E-01 | -0.080 | -0.252 | -0.180 | #N/A |
| TWIST1 | 5.45E-03 | 1.26E-04 | 3.04E-04 | 0.956 | 1.007 | 1.055 | track_C |
| VCAM1 | 3.35E-02 | 5.24E-02 | 1.17E-02 | 1.800 | 1.729 | 2.102 | track_B |
| WISP1 | 8.63E-01 | 8.93E-01 | 7.61E-01 | -0.053 | 0.048 | 0.114 | #N/A |

| | | | | | | | |
|---|---|---|---|---|---|---|---|
| WNT1 | 7.69E-01 | 6.77E-01 | 4.71E-01 | 0.008 | -0.010 | -0.012 | #N/A |
| WNT10B | 1.22E-01 | 2.34E-02 | 2.32E-02 | 0.487 | 0.649 | 0.793 | track_D |
| WNT3A | 8.93E-02 | 3.54E-02 | 1.56E-02 | -0.722 | -0.904 | -0.963 | track_K |
| WNT5A | 3.25E-01 | 2.95E-01 | 5.83E-01 | 0.274 | 0.264 | 0.154 | #N/A |
| WNT7B | 6.13E-01 | 1.00E-01 | 3.24E-01 | 0.173 | 0.344 | 0.259 | #N/A |

**Table S3:** Table of all differentially expressed microRNAs. Foldchange refers to log2 fold-change of each microRNA for that IPF stage versus control. Red boxes highlight the adjusted p-values that were below the significance threshold (0.1).

| **microRNA** | **IPF1_adj.p.val** | **IPF2_adj.p.val** | **IPF3_adj.p.val** | **IPF1_fc** | **IPF2_fc** | **IPF3_fc** |
|---|---|---|---|---|---|---|
| hsa-let-7a-5p | 1.00E+00 | 3.44E-02 | 2.67E-02 | 0.057 | -0.460 | -0.629 |
| hsa-let-7d-5p | 9.85E-01 | 3.54E-02 | 2.67E-02 | -0.207 | -0.416 | -0.558 |
| hsa-let-7g-5p | 1.00E+00 | 2.16E-01 | 5.61E-03 | -0.085 | -0.288 | -0.550 |
| hsa-let-7i-5p | 1.85E-01 | 1.85E-02 | 6.27E-02 | 0.500 | 0.527 | 0.543 |
| hsa-miR-1180 | 1.00E+00 | 1.21E-01 | 9.92E-02 | 0.149 | 0.530 | 0.621 |
| hsa-miR-125b-5p | 6.41E-01 | 5.99E-02 | 3.70E-01 | 0.294 | 0.578 | 0.390 |
| hsa-miR-126-3p | 3.60E-04 | 1.12E-05 | 8.50E-06 | -0.765 | -1.352 | -1.426 |
| hsa-miR-1260b | 1.45E-01 | 5.03E-02 | 1.60E-01 | -0.393 | -0.468 | -0.433 |
| hsa-miR-127-3p | 9.35E-03 | 3.07E-03 | 7.15E-03 | 1.766 | 1.810 | 1.746 |
| hsa-miR-1285-3p | 1.00E+00 | 5.46E-02 | 8.86E-01 | -0.010 | -0.949 | -0.074 |
| hsa-miR-1302 | 2.34E-01 | 2.18E-01 | 2.97E-02 | 0.604 | 0.513 | 0.915 |
| hsa-miR-130a-3p | 1.85E-01 | 2.44E-02 | 2.48E-01 | -0.438 | -0.432 | -0.444 |
| hsa-miR-132-3p | 6.06E-02 | 3.26E-02 | 8.15E-02 | 0.776 | 0.615 | 0.631 |
| hsa-miR-135a-5p | 1.63E-03 | 1.01E-03 | 2.77E-02 | -1.692 | -1.816 | -1.645 |
| hsa-miR-141-3p | 1.17E-01 | 8.77E-02 | 7.44E-01 | -0.882 | -0.536 | -0.245 |
| hsa-miR-144-3p | 5.21E-01 | 6.51E-02 | 8.42E-02 | 1.610 | 2.150 | 2.553 |
| hsa-miR-1537 | 1.17E-02 | 2.77E-03 | 1.84E-02 | -0.853 | -0.863 | -0.977 |
| hsa-miR-154-5p | 1.39E-01 | 2.26E-01 | 3.63E-02 | 0.616 | 0.541 | 0.856 |
| hsa-miR-155-5p | 6.03E-02 | 1.86E-02 | 2.94E-02 | 2.373 | 2.577 | 2.368 |
| hsa-miR-181a-5p | 6.09E-01 | 9.76E-03 | 2.39E-02 | -0.275 | -0.639 | -0.891 |
| hsa-miR-181b-5p+ hsa-miR-181d | 1.00E+00 | 6.54E-02 | 1.51E-01 | 0.046 | -0.346 | -0.403 |
| hsa-miR-181c-5p | 2.79E-01 | 2.44E-02 | 1.20E-01 | -0.336 | -0.445 | -0.557 |
| hsa-miR-182-5p | 3.16E-03 | 3.07E-03 | 7.15E-03 | 0.794 | 0.728 | 0.770 |
| hsa-miR-183-5p | 1.54E-02 | 1.43E-01 | 4.40E-02 | 0.659 | 0.444 | 0.521 |
| hsa-miR-185-5p | 6.03E-02 | 5.99E-02 | 1.72E-02 | 0.735 | 0.569 | 0.674 |
| hsa-miR-187-3p | 1.00E+00 | 7.16E-02 | 1.63E-01 | 0.179 | 0.630 | 0.622 |
| hsa-miR-199a-3p+ hsa-miR-199b-3p | 1.45E-01 | 1.28E-02 | 8.15E-02 | 0.630 | 0.878 | 0.731 |
| hsa-miR-199a-5p | 7.23E-03 | 3.35E-02 | 1.05E-02 | 0.878 | 0.762 | 0.983 |

| | | | | | | |
|---|---|---|---|---|---|---|
| hsa-miR-199b-5p | 6.03E-02 | 9.52E-04 | 5.86E-02 | 0.903 | 1.174 | 0.762 |
| hsa-miR-200a-3p | 7.03E-02 | 7.69E-01 | 8.42E-01 | -0.624 | -0.237 | -0.092 |
| hsa-miR-203 | 3.61E-02 | 1.77E-03 | 2.39E-02 | -0.831 | -1.167 | -1.133 |
| hsa-miR-205-5p | 8.14E-01 | 4.06E-03 | 1.01E-02 | 0.868 | 2.410 | 2.396 |
| hsa-miR-208a | 5.82E-01 | 5.03E-02 | 5.56E-01 | -0.287 | -0.607 | -0.230 |
| hsa-miR-20a-5p+ hsa-miR-20b-5p | 5.21E-01 | 6.53E-02 | 7.44E-01 | -0.239 | -0.366 | -0.123 |
| hsa-miR-21-5p | 2.11E-04 | 6.10E-07 | 4.46E-05 | 1.427 | 1.668 | 1.965 |
| hsa-miR-218-5p | 7.23E-03 | 8.28E-02 | 3.84E-02 | -1.013 | -0.843 | -0.991 |
| hsa-miR-219-1-3p | 2.85E-01 | 3.57E-01 | 6.10E-02 | 0.422 | 0.397 | 0.560 |
| hsa-miR-222-3p | 2.63E-02 | 3.44E-02 | 4.04E-01 | -0.745 | -0.509 | -0.315 |
| hsa-miR-223-3p | 1.17E-01 | 5.78E-02 | 8.76E-02 | -0.961 | -1.077 | -1.179 |
| hsa-miR-26a-5p | 9.55E-01 | 1.82E-01 | 8.79E-02 | -0.246 | -0.540 | -0.681 |
| hsa-miR-26b-5p | 8.62E-01 | 2.94E-01 | 7.24E-02 | -0.224 | -0.363 | -0.557 |
| hsa-miR-27b-3p | 6.95E-02 | 2.75E-02 | 5.01E-03 | 0.423 | 0.595 | 0.800 |
| hsa-miR-299-5p | 2.26E-01 | 7.24E-02 | 3.86E-02 | 0.489 | 0.530 | 0.684 |
| hsa-miR-29c-3p | 2.63E-02 | 1.77E-01 | 3.03E-01 | -0.825 | -0.509 | -0.442 |
| hsa-miR-30a-5p | 7.23E-03 | 1.19E-04 | 4.18E-03 | -0.968 | -1.337 | -1.327 |
| hsa-miR-30b-5p | 6.57E-02 | 7.17E-03 | 7.15E-03 | -1.131 | -1.431 | -1.603 |
| hsa-miR-30d-5p | 2.11E-04 | 2.38E-05 | 4.16E-04 | -1.456 | -1.563 | -1.555 |
| hsa-miR-30e-5p | 2.01E-01 | 3.46E-02 | 7.42E-01 | -0.567 | -0.438 | -0.219 |
| hsa-miR-3127-5p | 5.58E-01 | 9.98E-02 | 3.88E-01 | -0.432 | -0.667 | -0.423 |
| hsa-miR-3184-5p | 4.87E-01 | 6.03E-01 | 3.84E-02 | 0.509 | 0.413 | 0.883 |
| hsa-miR-323a-3p | 6.95E-02 | 2.07E-01 | 6.40E-02 | 0.757 | 0.580 | 0.887 |
| hsa-miR-335-5p | 1.00E+00 | 6.03E-02 | 2.94E-01 | -0.129 | -0.477 | -0.313 |
| hsa-miR-337-5p | 1.23E-01 | 1.16E-01 | 2.94E-02 | 0.685 | 0.656 | 0.946 |
| hsa-miR-338-3p | 2.11E-04 | 1.18E-04 | 2.98E-05 | -1.918 | -1.871 | -2.502 |
| hsa-miR-34a-5p | 1.57E-02 | 1.57E-02 | 1.01E-02 | 0.741 | 0.884 | 1.164 |
| hsa-miR-34c-3p | 1.00E+00 | 1.57E-02 | 4.22E-02 | 0.193 | 0.908 | 0.927 |
| hsa-miR-34c-5p | 1.00E+00 | 6.97E-02 | 7.27E-02 | 0.551 | 1.538 | 1.623 |
| hsa-miR-376a-3p | 2.72E-02 | 2.50E-03 | 1.02E-03 | 0.982 | 1.343 | 1.688 |
| hsa-miR-376c | 6.03E-02 | 2.44E-02 | 1.05E-02 | 0.677 | 0.773 | 1.054 |
| hsa-miR-377-3p | 2.63E-02 | 9.21E-04 | 5.01E-03 | 0.908 | 1.305 | 1.344 |
| hsa-miR-378d | 1.85E-01 | 5.78E-02 | 1.61E-02 | 0.902 | 0.857 | 1.002 |

| | | | | | | |
|---|---|---|---|---|---|---|
| hsa-miR-382-5p | 1.83E-02 | 2.87E-03 | 1.01E-02 | 1.157 | 1.196 | 1.369 |
| hsa-miR-409-3p | 2.46E-01 | 2.55E-01 | 8.15E-02 | 0.664 | 0.614 | 0.913 |
| hsa-miR-411-5p | 3.93E-01 | 2.94E-01 | 2.39E-02 | 0.493 | 0.529 | 0.876 |
| hsa-miR-423-5p | 9.50E-01 | 4.35E-02 | 1.60E-01 | -0.230 | -0.649 | -0.494 |
| hsa-miR-4286 | 1.00E+00 | 9.13E-01 | 6.40E-02 | 0.231 | 0.393 | 1.634 |
| hsa-miR-451a | 3.78E-02 | 3.69E-02 | 1.04E-01 | 2.455 | 2.317 | 1.833 |
| hsa-miR-455-5p | 5.77E-02 | 2.52E-01 | 4.25E-01 | -0.474 | -0.376 | -0.207 |
| hsa-miR-495 | 7.23E-03 | 2.77E-03 | 1.02E-03 | 1.233 | 1.234 | 1.547 |
| hsa-miR-506-3p | 4.27E-01 | 2.65E-01 | 8.07E-02 | 0.561 | 0.541 | 0.782 |
| hsa-miR-507 | 6.08E-01 | 4.81E-01 | 6.40E-02 | 0.542 | 0.447 | 0.801 |
| hsa-miR-509-3p | 6.09E-01 | 8.46E-01 | 9.76E-02 | 0.436 | 0.284 | 0.669 |
| hsa-miR-513b | 2.01E-01 | 2.79E-01 | 1.01E-02 | 0.645 | 0.435 | 0.851 |
| hsa-miR-518b | 6.99E-02 | 3.23E-02 | 3.16E-02 | -0.654 | -0.788 | -0.817 |
| hsa-miR-522-3p | 8.08E-01 | 2.84E-02 | 4.23E-02 | -0.330 | -0.863 | -0.922 |
| hsa-miR-543 | 7.93E-02 | 3.23E-02 | 2.67E-02 | 0.843 | 0.911 | 1.153 |
| hsa-miR-548g-3p | 1.31E-01 | 3.26E-02 | 1.83E-02 | 0.891 | 0.844 | 0.985 |
| hsa-miR-548v | 1.83E-01 | 6.91E-02 | 2.53E-01 | -0.526 | -0.598 | -0.440 |
| hsa-miR-592 | 3.34E-01 | 8.28E-02 | 3.71E-01 | -0.716 | -0.945 | -0.757 |
| hsa-miR-598 | 8.37E-01 | 5.03E-02 | 8.03E-02 | -0.247 | -0.507 | -0.539 |
| hsa-miR-630 | 1.00E+00 | 5.78E-02 | 6.27E-01 | -0.304 | -1.001 | 0.375 |
| hsa-miR-656 | 6.09E-01 | 7.78E-01 | 6.35E-02 | 0.386 | 0.296 | 0.761 |
| hsa-miR-874 | 3.13E-01 | 4.96E-01 | 2.39E-02 | 0.646 | 0.440 | 0.779 |
| hsa-miR-933 | 6.59E-01 | 1.71E-01 | 7.55E-02 | 0.437 | 0.535 | 0.637 |
| hsa-miR-96-5p | 1.74E-01 | 1.19E-01 | 1.48E-02 | 0.486 | 0.541 | 0.824 |
| hsa-miR-99a-5p | 8.43E-02 | 7.28E-03 | 1.12E-01 | 0.389 | 0.581 | 0.524 |

**Table S4:** A list of microRNAs and target genes in each stage of IPF. Symbols (*, †, or ‡) indicate genes regulated by their respective microRNAs.

## 1. MicroRNAs with increased expression and corresponding decreased target genes.

### IPF core microRNAs and genes

miR-127-3p, miR-21-5p†, miR-382-5p, miR-495

COBLL1†, DOCK5†, FAM126B†, GRPEL2†, ITSN2†, KAT6A†, MEF2A†, MKNK2†, NCOA3†, PFKFB2†, PIK3R1†, PLEKHA1†, RAPH1†, SASH1†, SESTD1†, SNRK†, SSFA2†, STAT3†, THOC2†, TMEM245†

### IPF1 microRNAs and genes

miR-127-3p, miR-21-5p†, miR-382-5p, miR-451a, miR-495

AGO2†, ARPP19, CDKN2D, CEBPB†, CLOCK†, COBLL1†, DOCK5†, EXOSC2, FAM126B†, FNIP1, GRPEL2†, HIPK3†, IL6R, ITSN2†, KAT6A†, MAPK1, MEF2A†, MKNK2†, MYO9A†, NCOA3†, NIPBL†, NSUN2†, PDHA2†, PFKFB2†, PIK3R1†, PKNOX1†, PLEKHA1†, PPARA†, PRKCE†, PROSER1†, RAPH1†, SASH1†, SESTD1†, SLC10A7, SNRK†, SSFA2†, STAT3†, STUB1†, THOC2†, TMEM245†, VEGFA†, WNK3†, WWC2†

### IPF2 microRNAs and genes

miR-127-3p, miR-155-5p*, miR-199b-5p, miR-205-5p, miR-21-5p†, miR-376a-3p, miR-377-3p, miR-382-5p, miR-451a, miR-495

ARHGEF12†, ARL8B*, ARPP19, BMPR2†, CARHSP1*, CCDC69, CDC42BPB*, CDKN2D, CDV3*, CEBPB*†, CFL2*, CNTROB, COBLL1†, CUX1*, CYP1A1*, CYP20A1, DOCK5†, DUSP8†, ECI1*, EGFR*†, ERGIC1*, FAM126B†, FAM177A1*, FLT1*, FRMD3, GATA6, GOLPH3*, GPD1L†, GRB10, GRPEL2†, HAL*, HERPUD2†, HSPA12B, BA57, IL6R, INPP5A*, ITSN2†, KAT6A†, KCTD3*, LIMCH1†, LNX2*, LTN1*, MAPK1, MAPK4, MARCH2, MEF2A*†, MGAT4A†, MIA2*, MKNK2†, MMAB, MUT*, MYO10*, MYO9A†, NANOS1, NCKAP1*, NCOA3†, NDUFS2, PACSIN3*, PAM16*, PARD6B, PCGF2†, PELI2, PFKFB2†, PHGDH*, PIK3R1*†, PLEKHA1†, PNPLA8*, POLR2C*, PPL*, PPM1L†, PRKAR2A*, PROSER1†, PTPRM, PURB†, RAB11FIP1, RAB21, RAB3IP*, RAB5A, RAB6A*†, RAD1*, RAPGEF2*, RAPH1*†, RCOR1*, SASH1†, SEC24B*, SESTD1†, SLC26A2†, SLC35G2, SMARCD2*, SNRK†, SORT1, SSFA2†, SSU72*, STARD7, STAT3*†, TAL1, TBC1D14*, TBCA*, THOC2†, TMEM245†, TRAPPC6B, UBE2B, UBXN2B*, UVRAG, VEGFA†, VPS26A†, WWC1*, WWC2†, YARS*, YES1, YWHAH, ZNF148*, ZNF669, ZNF736

### IPF3 microRNAs and genes

miR-127-3p, miR-155-5p*, miR-205-5p, miR-21-5p†, miR-34a-5p‡, miR-376a-3p, miR-376c, miR-377-3p, miR-378d, miR-382-5p, miR-495, miR-543

ACSL1‡, AMD1, ARHGEF12†, ARL8B*, ATP5S‡, ATXN1L‡, BCL2L13‡, BFAR‡, BMPR2†, BNIP3‡, CARHSP1*, CCDC69, CCND3‡, CD93, CDH13*, CDV3*, CFL2*, CLTB‡, CMSS1*, CNTROB, COBLL1†, CTIF‡, CYP1A1*, CYP51A1*‡, DOCK5†, EEF1E1*, EFNB1‡, EGFR*†, ELOVL7†, ERGIC1*, ETF1, FADS1*, FAH‡, FAM126B†, FAM177A1*, FKBP1A, FLT1*, FRMD3, GRPEL2†, GYG1‡, H3F3B‡, HAL*, HAX1*, HERPUD2†, HIRIP3‡, HSD17B7*, HSPA12B, IBA57, IL6R‡, INPP5A*, IPO7, ITGA5, ITSN2†, JPH1†, KAT6A†, LDLR, LIMCH1†, LNX2*, MAGI1‡, MAPK4, MARCH2, MEF2A*†, MEGF9†, MFN2‡, MKNK2†‡, MMAB, MYO10*, MYO1C‡, NANOS1, NCKAP1*, NCOA3†, NDUFA12, PALD1*, PAM16*, PARD6B, PCGF2†, PELI2, PFKFB2†, PIK3R1*†, PLEKHA1†, POLR2C*, PPL*, PPP1R11‡, PRKAR2A*, PTPRM, PURB†, RAB11FIP1, RAB21, RAB6A*†, RAPH1*†, RCOR1*, RPIA‡, SASH1†, SEC24B*, SESTD1†, SETD3‡, SLC35G2‡, SMARCD2*, SNRK†, SNX12‡,

SORT1‡, SPRY2†, SPTBN1‡, SQLE, SSFA2†, SSH2*, SSU72*, STARD7, STAT3*†, TAL1, THOC2†‡, TJP2‡, TMEM2†, TMEM245†, TOMM20*, TPRG1L†, TTLL12‡, UBA2*‡, UBE2B, UBE2J2*, UBQLN1*, UBXN2B*‡, VAMP2‡, VAPA, VPS26A†, WWC1*, YARS*, YES1, YWHAH, ZNF736

## 2. MicroRNAs with decreased expression and corresponding increased target genes.

**IPF1 microRNAs and genes**
miR-126-3p, miR-1537, miR-203, miR-222-3p, miR-29c-3p*, miR-30a-5p

COL10A1*, COL15A1*, COL1A1*, COL1A2*, COL3A1*, COL5A2*, CXCL12, KCNN4, MMP2*, MMP7, PHLDA2, PTGFRN, SELE, TGFBI, TUBB3, VCAM1

**IPF2 microRNAs and genes**
let-7a-5p, let-7d-5p*, miR-130a-3p, miR-1537, miR-181a-5p, miR-181c-5p, miR-222-3p, miR-30e-5p, miR-423-5p, miR-518b, miR-522-3p

APOBEC3C, CDKN2A, CERCAM, COL16A1, COL3A1*, COL5A2, CST5, HAS2, HLA-DOA, LRRC17, MMP1, SELE, SOX2, TFAP2A, TMEM45A, TRIM2, TWIST1, UCHL1

**IPF3 microRNAs and genes**
let-7a-5p, let-7d-5p*, let-7g-5p†, miR-1537, miR-181a-5p, miR-218-5p, miR-518b, miR-522-3p

ADAM12, CCDC80, CCL22, CCNB2, CCR7, COL16A1, COL1A2†, COL3A1*, CST5, CYP24A1, EGR3, EPHB2, FKBP10, FN1†, HAS2, ITM2C, LOXL2, LRRC17, MMP14, MMP2, MSC, PTGFRN, SFRP2, SMO, SOX2, TEX9, TMEM45A, TRIM2, TWIST1, UCHL1, VCAM1

## References

1. Ashcroft T, Simpson JM, Timbrell V. Simple method of estimating severity of pulmonary fibrosis on a numerical scale.. *J. Clin. PathTrackol.* 1988;41(4):467–470.

2. Schulz MH et al. DREM 2.0: Improved reconstruction of dynamic regulatory networks from time-series expression data. *BMC Syst. Biol.* 2012;6:104.

3. Ding J, Hagood JS, Ambalavanan N, Kaminski N, Bar-Joseph Z. iDREM: Interactive visualization of dynamic regulatory networks. *PLoS Comput. Biol.* 2018;14(3):e1006019.

4. Bengio Y, Frasconi P. An Input Output HMM Architecture. *Adv. Neural Inf. Process. Syst. 7* 1995;427–434.

5. Bar-Joseph Z, Gitter A, Simon I. Studying and modelling dynamic biological processes using time-series gene expression data. *Nat. Rev. Genet.* 2012;13(8):552–564.

6. Reyfman PA et al. Single-Cell Transcriptomic Analysis of Human Lung Provides Insights into the Pathobiology of Pulmonary Fibrosis. *Am. J. Respir. Crit. Care Med.* [published online ahead of print: December 15, 2018]; doi:10.1164/rccm.201712-2410OC

7. Qin XF, Reichlin A, Luo Y, Roeder RG, Nussenzweig MC. OCA-B integrates B cell antigen receptor-, CD40L- and IL 4-mediated signals for the germinal center pathway of B cell development. *EMBO J.* 1998;17(17):5066–5075.

8. Bauer Y et al. A novel genomic signature with translational significance for human idiopathic pulmonary fibrosis. *Am. J. Respir. Cell Mol. Biol.* 2015;52(2):217–231.

9. McDonough JE et al. Gene correlation network analysis to identify regulatory factors in idiopathic pulmonary fibrosis. *Thorax* 2019;74(2):132–140.

10. Vukmirovic M, Kaminski N. Impact of Transcriptomics on Our Understanding of Pulmonary Fibrosis. *Front. Med.* 2018;5:87.